Low Conductive Electrodeposited Poly(2,5-dimethoxyaniline) as a Key Material in a Double Lateral Heterojunction, for Sub-ppm Ammonia Sensing in Humid Atmosphere

Mickaël Mateos, Marie-Donga Tchangaï, Rita Meunier-Prest, Olivier Heintz, Frédéric Herbst, Jean-Moïse Suisse, Marcel Bouvet

M. Mateos et al., ACS Sensors 2019, DOI 10.1021/acssensors.9b00109

Graphical abstract

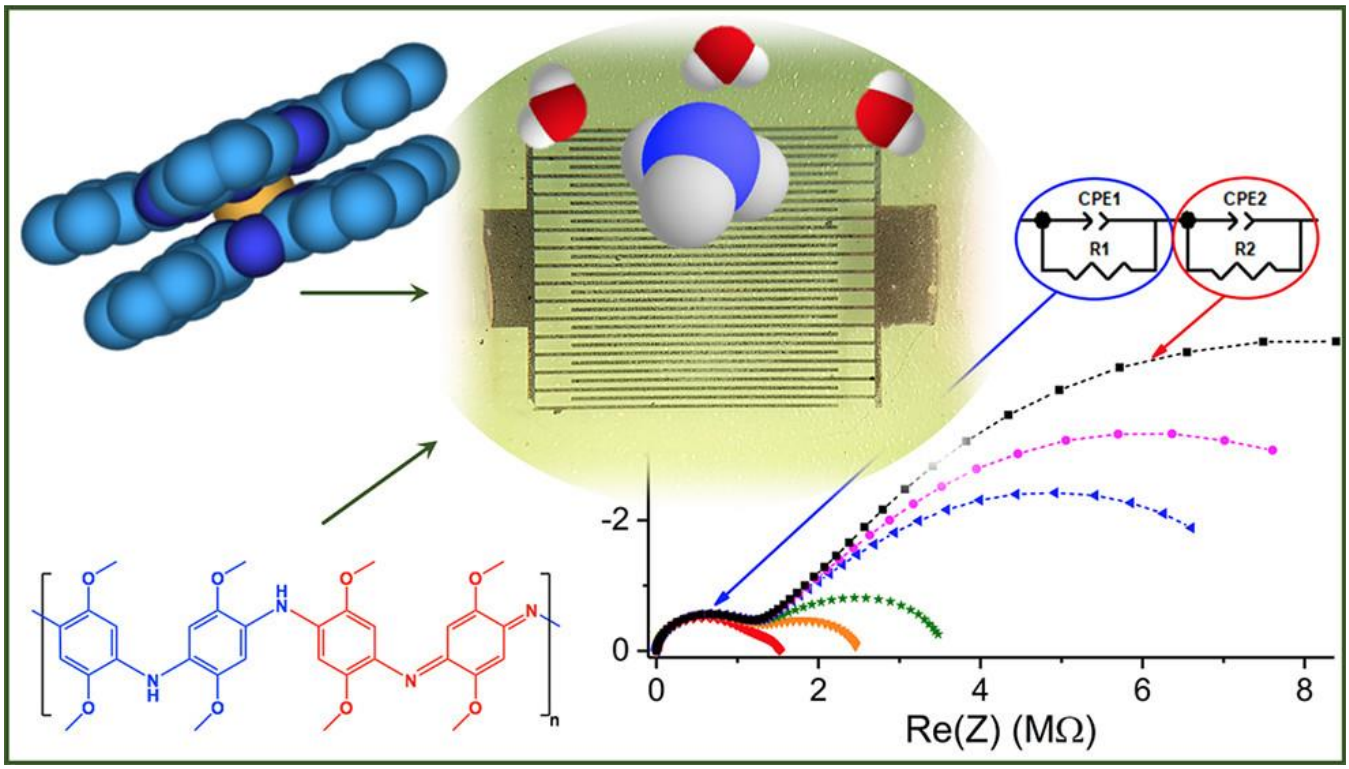

M. Mateos et al., ACS Sensors 2019, DOI 10.1021/acssensors.9b00109

The low conductive electrodeposited poly(2,5-dimethoxyaniline) as a key material in a double lateral heterojunction, for sub-ppm ammonia sensing in humid atmosphere

Mickaël Mateos[a], Marie-Donga Tchangaï [a], Rita Meunier-Prest[a]*, Olivier Heintz[b], Frederic Herbst[b], Jean-Moïse Suisse[a], Marcel Bouvet[a]*.

[a]Institut de Chimie Moléculaire de l'Université de Bourgogne (ICMUB), UMR CNRS 6302, Université Bourgogne Franche-Comté, 9 avenue Alain Savary, 21078 Dijon cedex, France. Tel: +33-380-396-086; E-mail: marcel.bouvet@u-bourgogne.fr, rita.meunier-prest@u-bourgogne.fr

[b]Laboratoire Interdisciplinaire Carnot de Bourgogne (LICB), UMR CNRS 6303, Université Bourgogne Franche-Comté, 9 avenue Alain Savary, 21078 Dijon cedex, France

KEYWORDS. Electrochemistry, conducting polymer, polyaniline, impedance spectroscopy, conductometric transducer, relative humidity, ammonia sensor.

ABSTRACT: We present a new device called double lateral heterojunction (DLH) as ammonia sensor in humid atmosphere. It combines polyaniline derivatives in their poor conducting state with a highly conductive molecular material, lutetium bisphthalocyanine, $LuPc_2$. The polyaniline and poly(2,5-dimethoxyaniline) are electrodeposited on ITO interdigitated electrodes, leading to an original device that can be obtained only by electrochemistry and not by other solution processing techniques. Both polymers lead to highly conducting materials that require a neutralization step before their covering by $LuPc_2$. While the device based on polyaniline shows an ohmic behavior, the non-linear I-V characteristics of poly(2,5-dimethoxyaniline) – based DLH proves the existence of energy barriers at the interfaces, as demonstrated by impedance spectroscopy. It exhibits a particularly interesting sensitivity to ammonia, at room temperature and in a broad relative humidity range. Thanks to its higher energy barriers, the poly(2,5-dimethoxyaniline)/$LuPc_2$ DLH is the most sensitive device with a limit of detection of 320 ppb. This work paves the way for the use of substituted polyanilines in conductometric sensors not only in the field of air quality monitoring but also in the field of health diagnosis by measurement in human breath.

Conductometric gas sensors are mostly resistors using inorganic materials, such as metallic oxides. However, molecular material – based resistors also reveal to be highly sensitive devices, with the advantage to operate at room temperature. Beside organic resistors, field-effect transistors (OFET) and p-n junctions were used as conductometric transducers. These devices were developed after their inorganic counterparts. In most of the cases, complex apparatus are necessary, which involve high vacuum and/or high temperature processes. On the contrary, solution processing techniques are particularly suitable for large areas and low cost processes.[1,2] Metal oxide – based heterojunctions were considerably studied as gas sensors.[3] Heterojunctions between inorganic and organic materials were also used as gas sensors, e.g. towards liquefied petroleum gas, with n-CdS/PANI.[4] Discoid SnO_2 with reduced graphene oxide was also used to detect NO_2.[5] Conducting polymers, polyaniline (PANI), polypyrrole and polythiophene, were associated with nanostructured metal oxides to detect a series of VOCs, leading generally to better performances than with the isolated components in resistors.[6-9] We can also cite phthalocyanines combined with ZnS.[10] Organic Schottky diodes were widely reported as gas sensors,[11] unlike heterojunctions combining two molecular materials. We can mention phthalocyanine-based p-n heterojunctions,[12] which behave electrically as classical p-n diodes, and a particular conductometric transducer, called MSDI, for Molecular Semiconductor – Doped Insulator heterojunction.[13,14]

Besides, beyond its synthetic interest,[15] electrochemistry became highly popular to modify electrode surfaces.[16] In the case of conducting polymers, electrochemistry ensures the synthesis and the preparation of materials in a unique step, as exemplified by phthalocyanine-polypyrrole hybrid materials used as sensing material for the detection of NH_3.[17] In the case of polyanilines, the control of their conducting state, related to their doping state, determines their electrical and optical properties.[18] The electronic and physico-chemical properties of conducting polymers are highly dependent on the nature of substituents. Thus, polyanilines were synthesized from aniline bearing electron-withdrawing and electron-donating substituents such as fluorine atoms[19] and alkoxy groups.[20]

In this paper, we report on a new device called double lateral heterojunction (DLH) that implies a double interface between two molecular materials: a poor conductive polymer around the electrodes and a molecular semiconductor, the lutetium bisphthalocyanine, $LuPc_2$, as a top layer (Figure 1). Actually, we reported recently a first example of DLH, using the poly(tetrafluoroaniline), PTFANI, starting from tetrafluoroaniline.[21] The main drawback with PTFANI was the difficulty to obtain homogeneous films, due to its insulating nature. Among phthalocyanines, $LuPc_2$, because of its radical nature, exhibits a

unique high intrinsic conductivity and a particularly high sensitivity to redox active species.[13] We develop two DLH differing in the polymer electroplated on ITO interdigitated electrodes (IDE): the poly(2,5-dimethoxyaniline) (PDMA) and the non-substituted polyaniline (PANI). Thanks to the electrochemical method, the polymer is deposed selectively onto the electrodes and not on all the substrate area. After vacuum evaporation of $LuPc_2$, the devices consist in DLH (Fig. 1). They were characterized thanks to electrical measurements like impedance spectroscopy and current-voltage characteristics, I(V). Finally, we compared the sensing properties of PANI-DLH and PDMA-DLH through ammonia sensing experiments in humid atmosphere.

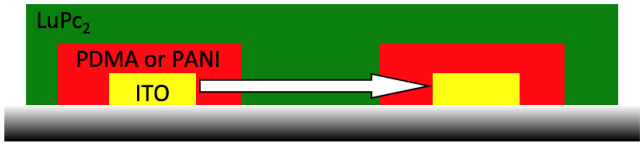

Figure 1. *Schematic view of the double lateral heterojunction (DLH); the arrow indicates the main channel for charge carriers.*

Experimental section

Chemicals

2,5-Dimethoxyaniline (DMA), 70% perchloric acid and potassium hydroxide were purchased from Sigma Aldrich and absolute ethanol (analaR normapur) was purchased from Carlo Erba. Aniline (Aldrich) was distilled at a boiling temperature of 120 °C under the reduced pressure before use. Ammonia gas, at 985 ppm and 98 ppm (mol/mol) in synthetic air, and synthetic air were used from standard gas cylinders, purchased from Air Liquide, France. Lutetium bisphthalocyanine ($LuPc_2$) was synthesized according to a previously reported method.[22]

Electrochemical methods

All electrochemical experiments were performed with a PGSTAT302N (Metrohm) potentiostat and the collected data analyzed using Nova® 2.1 software. Cyclic voltammetry (CV) and chronoamperometry (ChA) were carried out by means of a three-electrode setup consisting of an ITO plate or ITO interdigitated electrodes (IDE, deposited onto a 1 x 1 cm² floated glass substrate and separated by 75 µm with 50 nm thickness) as working electrode, a platinum wire as counter electrode and a saturated calomel electrode (SCE) as reference electrode. Potentials were reported versus SCE. PANI films were deposited on ITO plates by ChA at 1 V in a solution of 0.15 M aniline in 2 M $HClO_4$ (consumed charge of 415 mC.cm^{-2}), then rinsed with 0.2 M $HClO_4$, absolute EtOH and dried under vacuum at room temperature. They were also deposited on IDE by ChA at 0.9 V (consumed charge of 115 mC.cm^{-2}) under similar conditions. PDMA films were deposited on ITO plates by CV from -0.3 V to 1 V at a scan rate of 40 mV.s^{-1}, in a 50 mM DMA solution in 2 M $HClO_4$. The CV was stopped at 0 V after consuming 1 C.cm^{-2}, then the polymer films were rinsed with 0.2 M $HClO_4$, absolute EtOH and dried under vacuum at room temperature. They were also deposited on IDE in the same conditions but with a consumed charge of 250 mC.cm^{-2}. To obtain their neutral forms the films were rinsed with 1 mM KOH, water and dried under vacuum at room temperature.

SEM images and XPS analysis

SEM images were performed with a scanning electronic microscope JEOL JSM6400F with 2 kV of acceleration voltage. XPS analysis of the polymer films was performed on a SIA100 spectrometer (Cameca Riber apparatus) using non-monochromated Al Kα X-ray source (1486.6 eV photons). All spectra were calibrated using the normalized In($3d_{5/2}$) XPS signal from In_2O_3 at 444.9 eV[23] and all deconvolutions were performed using contributions with a nearly constant width at half maximum (± 0.2 eV).

Electrical and chemosensing measurements

The top layer was coated over the neutralized polymer sublayer prepared on IDE, by sublimation of $LuPc_2$ in an UNIVEX 250 thermal evaporator (Oerlikon, Germany), under secondary vacuum (ca. 10^{-6} mbar), by heating in a temperature range of 400-500 °C, at a rate of 1 Å.s^{-1}. Impedance data were obtained using a Solartron SI 1260 impedance analyzer. The frequency range was 10 Hz to 10 MHz with a fixed ac oscillation amplitude of 300 mV and a bias ranging from 0 V to 10 V. A commercial software Zview from Ametek was used for impedance data fitting and parameter extraction. The apparatus used for NH_3 exposure, at different relative humidity (RH) values, was described previously.[24] The total flow was in the range 0.5-0.55 NL.min^{-1} depending on ammonia concentration and the volume of the test chamber was 12 cm^3. Gas sensing experiments were carried out in a dynamic way, by alternating 4 min-long rest periods and 1 min-long exposure periods.

Results and Discussion

Film formation

The electrodeposition of PDMA on ITO electrodes was carried out by cyclic voltammetry in an acidic solution containing the monomer (Figure 2).

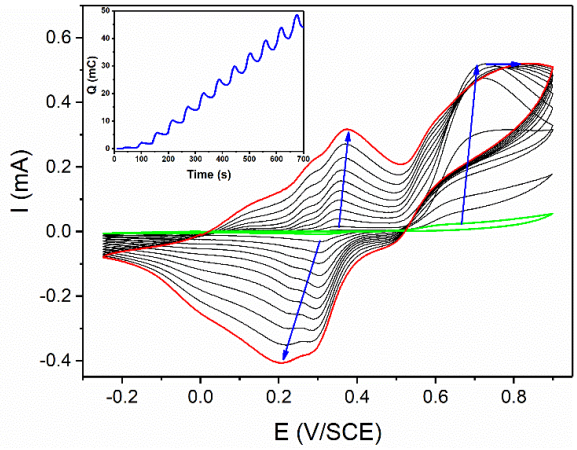

Figure 2. *Cyclic voltammogram of 50 mM DMA in 2 M $HClO_4$ on an ITO electrode, at 0.04 V.s^{-1}. Consumed charge in inset.*

DMA was irreversibly oxidized at 0.62 V. Repetitive scanning leaded to a new redox system, at around 0.37 and 0.2 V, attributed to the polymer formation.[25,26] Its intensity and the corresponding charge consumed (inset in Figure 2) grew rapidly with the number of scans. This was characteristic of a polymer having a good conductivity like PANI.[20] Previous EQCM results revealed a partially protonated emeraldine form with a doping ratio of 1 ClO_4^- / 2 DMA units.[20]

SEM images and XPS analysis

PDMA films electrodeposited on ITO plates had a broccoli shape structure (Figure 3).[27] This porous structure can be explained by the high conductivity of PDMA in its emeraldine salt form that enabled a fast growth on itself, as previously reported for PANI, which lead to fibers of a few hundred nanometers in length.[21]

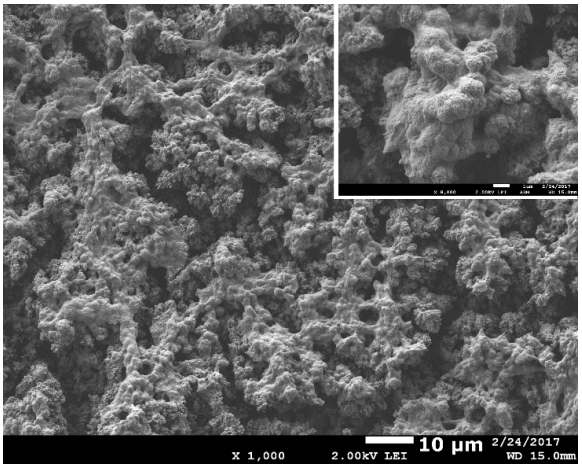

Figure 3. *SEM images of PDMA on ITO plates with a zoom (x8) in inset.*

The atomic ratio has been calculated from XPS spectra, using peak areas of C(1s), N(1s), O(1s) and Cl(2p) (N(1s) used as a reference, Figure S1). The C/N ratio of 8.4 was closed to the expected value of 8. The Cl/N ratio (0.7) demonstrates the presence of ClO_4^- counterions that indicates an important acid-base doping (protonation of amine/imine bridges). Furthermore, after subtracting the oxygen contribution from the two methoxy groups, the obtained O/Cl ratio (4) matched with ClO_4^- anions. The O(1s), Cl(2p) and C1s spectra are analyzed in Figure S2, S3 and S4, respectively. The deconvolution of N(1s) spectrum showed three components at 399.4, 401 and 403.5 eV, that can be attributed to the neutral amine, the protonated imine and the protonated amine, respectively (Figure 4a).[28-32] It is worth noting that, in our case, the neutral imine peak, expected at 398 eV,[33,34] was absent because all imine bridges were protonated. The acid-base doping was calculated by addition of the contributions of the protonated molecules at 401 and 403.5 eV. Charged species rates of 52% for PANI and 54% for PDMA were obtained. This was lower than the chlorine ratio obtained from XPS semi-quantitative analysis (0.7) because the Cl/N ratio also provided for traces of electrolyte not fully eliminated by the rinsing step with absolute EtOH. Otherwise, we demonstrated that PDMA and PANI had a -N= / -NH- ratio near to 1 in accordance with their emeraldine salt form.

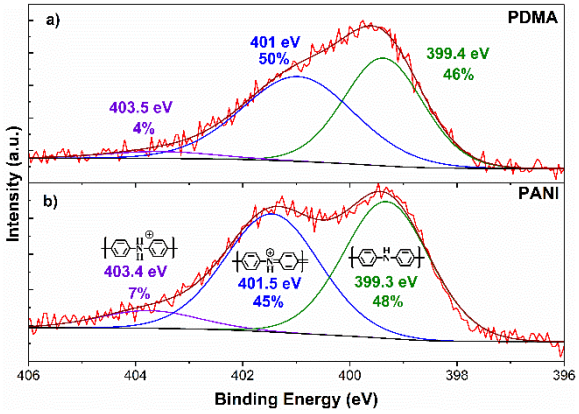

Figure 4. *N(1s) XPS high resolution spectra of a) PDMA, b) PANI films electrodeposited on ITO plates.*

Electrical properties

Inspired by the behavior of MSDI that include a low conductive sublayer, we decided to build heterojunctions, with PANI and PDMA in their low conductive form. Therefore, 1 µm thick polymer films of PDMA and PANI were electrodeposited on IDE, then neutralized by KOH, leading to their poor conductive state (emeraldine base form). A $LuPc_2$ upper layer was then added by vacuum sublimation to obtain DLH (Figure 1). The normalized I(V) characteristics of PDMA/$LuPc_2$ DLH, defined as the ratio of the current with its maximum value at 10 V, showed a non-linear behavior compared to the ohmic characteristic of a $LuPc_2$ resistor (Figure 5).

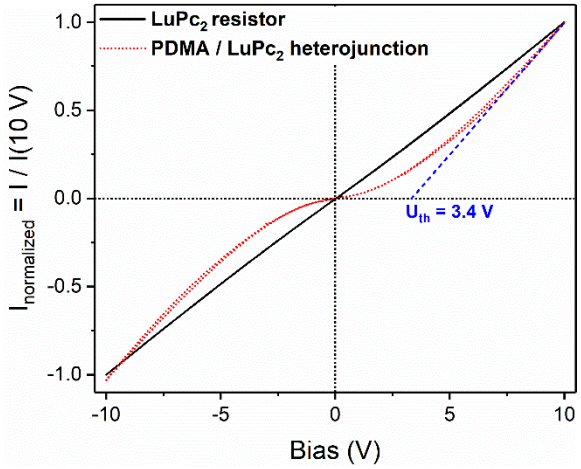

Figure 5. *Normalized I(V) characteristics in ambient atmosphere of a $LuPc_2$ resistor and a PDMA – DLH with the threshold voltage, U_{th}.*

This new lateral configuration forces the charges to cross twice the ITO/polymer and polymer/$LuPc_2$ interfaces, and creates energy barriers. The threshold voltage, U_{th}, provides an evaluation of the non-linear character of the PDMA – DLH. It is determined by extrapolation to zero of the tangent to the curve

at high bias (Figure 5). The obtained value of 3.4 V was higher than that of the poly(2,3,5,6-tetrafluoroaniline) (PTFANI)-based device (threshold voltage of 2 V calculated from ref. [21]). Despite the lower current in the PANI/$LuPc_2$ heterojunction (2 µA at 10 V, Figure S5) than in the $LuPc_2$ resistor (20 µA at 10 V), this device kept an ohmic I(V) characteristic, suggesting that all the interfaces formed ohmic contacts.

We explored the transport properties thanks to impedance spectroscopy, a conventional technique in electrochemistry, with recently growing applications in organic electronics.[35,36] Thereafter, we will discuss the complex plane representation, called the Nyquist plot, of the impedance Z defined as: Z = Re(Z) + jIm(Z), where Re(Z) and Im(Z) are the real and imaginary parts of Z, respectively. As shown in Figure 6, Nyquist plots of PDMA – DLH exhibited two intermixed non-ideal semicircles, which have different behaviors depending on the bias. The first one, at high frequency (HF), was practically independent of the bias, whereas the second one, at low frequency (LF), collapsed as the bias increased. It is worth noting that the $LuPc_2$ resistor exhibits only one semicircle unaffected by the bias. This means that the electrical properties of the resistor remain constant,[37] suggesting that the charge transport is dominated by the bulk material, and not by interfacial traps.[38] In the PDMA – DLH, when focusing on the diameter of the LF semicircle, the major part of the collapse occurred when the bias was lower than 3 V. This bias corresponds to the abovementioned threshold voltage of 3.4 V, deduced from the I(V) curves (Figure 5). Our working assumption, supported by previous studies,[37,39] was that, at low bias, the LF semicircle represents the interfacial behavior, whereas the HF semicircle represents properties from the bulk materials. For the present heterojunctions, with two non-ideal semicircles, the data were modeled by an equivalent circuit consisting of two R_i-CPE_i elements in series (Figure 6). A constant-phase element (CPE_i) can be regarded as an imperfect capacitor[40] of which the impedance Z_{CPEi} is defined as follows (equation 1):

$$Z_{CPEi} = \frac{1}{Q_i*(j\omega)^{\alpha_i}} \qquad (1)$$

with $\omega = 2\pi f$, where f is the frequency, Q_i the non-ideal capacitance, and α_i a value between 0 and 1 that reflects the non-ideality of the capacitive element.[36]

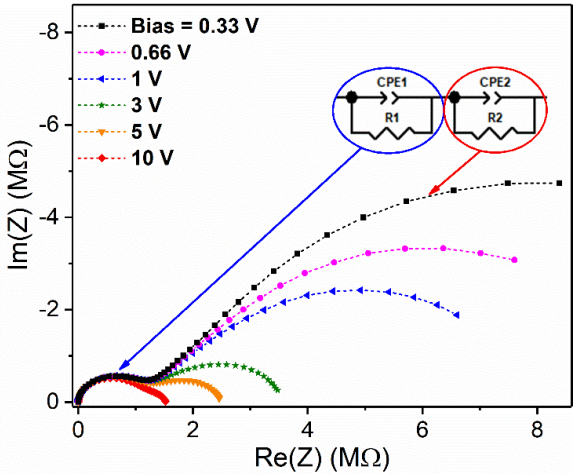

Figure 6. *Nyquist plot as a function of the bias (0.33 V to 10 V) of a PDMA – DLH, with the equivalent circuit for data modelling in inset.*

When $\alpha_i = 1$, a CPE corresponds to an ideal capacitor. As expected from the Nyquist plots, all the parameters (R_1, Q_1 and α_1) of the R_1-CPE_1 element remain nearly constant with the bias (Figure 7). This confirms that part of the properties of the bulk materials are modeled by this element. The collapse of the second semicircle observed in the Nyquist plot (Figure 6) results from the decrease of R_2

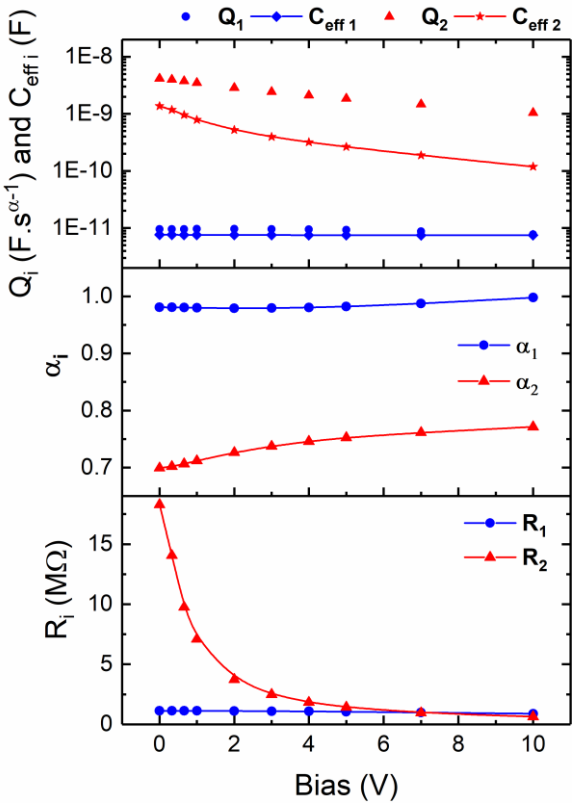

Figure 7. *Variations of the extracted circuit parameters as a function of the bias for PDMA – DLH.*

with the bias. This resistance is the key parameter to explain the energy barrier abovementioned and the non-linear behavior observed in the I(V) characteristics.

Indeed, the strong non-linear behavior (Figure 5) observed with PDMA sublayers results from the high value of R_2 at low bias (Figure 7). To be more specific, R_2 decreased from 18.3 MΩ to 0.6 MΩ and R_1 remained stable at 1.1 MΩ. The large part of the R_2 drop occurred for bias below 3 V, which corresponds to the threshold voltage of 3.4 V (Figure 5). To confirm that the interfacial phenomena were mainly represented by the R_2-CPE_2 element associated with the LF semicircle, we calculated the effective capacitance C_{effi}, (equation 2), of the R_i-CPE_i element (Figure 7) referring to a reported method.[41]

$$C_{eff\,i} = R_i^{\frac{1}{\alpha_i}-1} * Q_i^{\frac{1}{\alpha_i}} \qquad (2)$$

Actually, the parameter Q_i has no physical sense because its unit depends on α_i. It is worth noting that a R-C element attributed to an interfacial behavior should have a larger capacitance than the bulk capacitance, because an interfacial layer should have a smaller thickness compared to that of the device.[39] It appeared that C_{eff1} had a constant value of 8 pF whereas C_{eff2} declined from 1.4 nF at 0 V to 120 pF at 10 V, which is hundreds time higher than C_{eff1}. Furthermore, the PANI – DLH that exhibited an ohmic characteristic (Figure S5) displays a Nyquist plot with essentially one semicircle, as the second one was scarcely visible, reflecting the absence of interfacial energy barrier (Figure S6). Indeed, R_2 decreased from 970 kΩ at 0 V to 474 kΩ whereas R_1 remained almost stable at 1 MΩ (Figure S7). So R_2 was lower than R_1 whatever the bias. It means that interfacial barriers play a minor role in the electrical transport in the device, which is corroborated by its ohmic behavior. All these observations confirmed our starting hypothesis that the R_2-CPE_2 block, associated to the LF semicircle, modeled the role of the interfaces.

Gas sensing

Under exposure to NH_3 (Figure 8), the PDMA – DLH showed a current drop, which demonstrated that the transport properties are governed by positive charge carriers. The current decrease depended on the NH_3 concentration whatever the RH. The ΔI response, corresponding to the difference between the current at the end of the exposure phase I_f (1 min) and that of the recovery phase I_0 (4 min) was not linear in this NH_3 concentration range. Indeed, at 50% RH, ΔI went from -14 nA at 90 ppm NH_3 to -5.5 nA at 10 ppm. This suggested that the sensor worked in overloaded regime. All along this experiment, the I_0 value decreased with the RH value, but at each RH value I_0 was very stable during the exposure-recovery cycles. The device exhibited the same behavior when exposed to different RH values without NH_3 (Figure S8). We also studied the devices at lower NH_3 concentrations, between 1 and 9 ppm, at 50% RH (Figure 9).

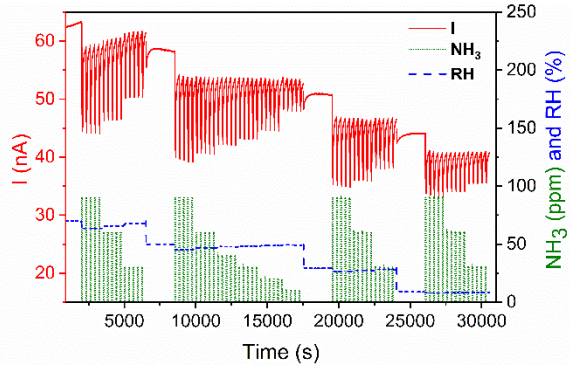

Figure 8. *Current response of PDMA – DLH exposed to NH_3, in humid air, from 70% RH to 10% RH, during exposure/recovery cycles (1 min / 4 min).*

The sensor continued to show a large current decrease, depending on the NH_3 concentration, with a stable current baseline. The ΔI value at 1 ppm was 1 nA, with a good signal-to-noise ratio, suggesting that the limit of detection (LOD) was not reached yet. The relative response, RR, defined in equation 3 from the mean value over four exposure / recovery cycles at each NH_3 concentration, reached 29% at 90 ppm NH_3, against 7%, for the PANI – based device.

$$RR\ (\%) = \frac{|I_f - I_0|}{I_0} * 100 \qquad (3)$$

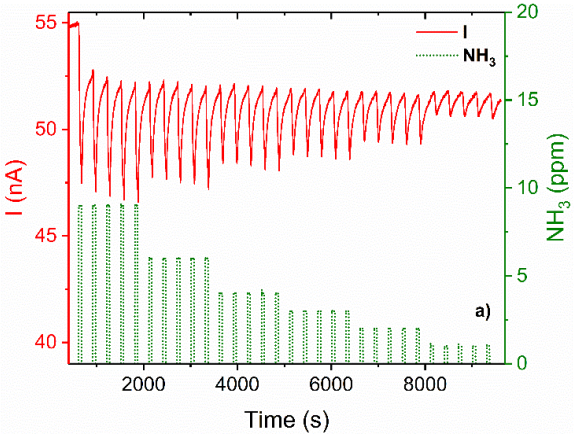

Figure 9. *Current response of a PDMA – DLH exposed to NH_3 (9, 6, 4, 3, 2 and 1 ppm), in air at 50 % RH, during exposure / recovery cycles (1 min / 4 min).*

The sensitivity, S, defined as the local slope of the curve RR = f([NH_3]) (Figure 10), was better at low concentrations than at high concentrations. In the overloaded regime (40 – 90 ppm), S was 0.12 %.ppm^{-1}, but at concentrations lower than 10 ppm, S rose up to 1.85 ± 0.17 %.ppm^{-1}. This increase of the sensitivity at low concentration suggested a Langmuir-like behavior. The data were fitted by the Langmuir adsorption isotherm (R^2 = 0.992).[42] In principle, the device could have an even greater sensitivity at low concentrations. Indeed, below 1 ppm, the modeling equation is reduced to a linear function whose slope (2.23 %.ppm^{-1}) represents the maximum theoretical sensitivity of the device. The LOD was calculated from I_0 and the noise, N, both graphically determined at 1 ppm on the curve I(t) (Figure 9) (equation 4):

$$LOD = \frac{3N}{S * I_0} \qquad (4)$$

With N being 0.1 nA and I_0 51.7 ± 0.2 nA, a LOD of 314 ± 29 ppb was calculated. It is important to remember that, in Europe, the daily exposure limit in NH_3 is 20 ppm.[43] These values demonstrate that this device is suitable for the detection of NH_3 at low concentrations.

We repeated the same experiments with the PANI – DLH (Figure 10). Compared to the PDMA – DLH, it exhibited a smaller RR value of 7.2 % at 90 ppm because of its poor ΔI response and its high I_0 value. Despite the instability of I_0 that explained the break in the RR curve between 10 and 20 ppm, we determined a sensitivity of 0.14 %.ppm^{-1} at low NH_3 range (< 9 ppm). The great sensing properties of the PDMA – DLH come from the energy barriers of the different interfaces, emphasized by the previous electrical measurements. By polarizing the sensor with a bias lower than the threshold voltage (bias of 1 V against U_{th} of 3.4 V), the current is limited by the charge

transfer at the interface. It provides an improvement of the sensitivity of the PDMA – DLH compared to that of devices with an ohmic behavior, as previously demonstrated for MSDI.[24]

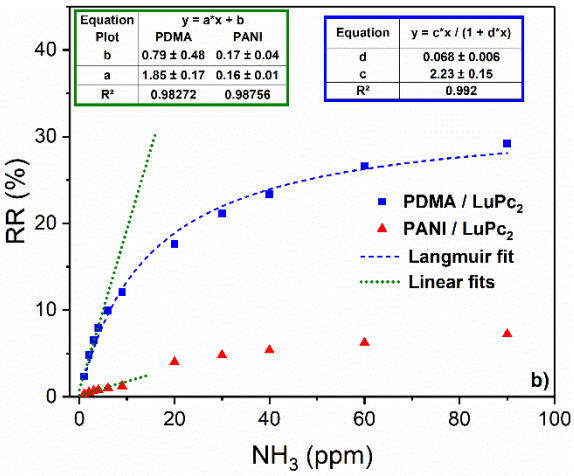

Figure 10. *Relative response of PDMA – DLH and PANI – DLH as a function of the NH_3 concentration in the 1-90 ppm range, in air at 50 % RH. The data of the linear fits for both devices (green table) and of the Langmuir modelling for the PDMA-DLH (blue table) are given in insets.*

The sensitivity of the PDMA – DLH is comparable to this of n-type MSDI[44] and better than that of a previously reported p-type conductometric device, the PTFANI – based DLH (Table 1).[21] Other NH_3 sensors operating at room temperature exhibited a sensitivity in the same range, such as resistors made from reduced graphene oxide (rGO) associated to Co_3O_4 nanofibers[45] or to PANI,[46] with a sensitivity of 1 %.ppm^{-1}. However, the latter was studied in dry air whereas the first one was studied only at 40% RH. Besides, inorganic-based sensors can exhibit a higher sensitivity, but they operate at high temperatures, e.g. at 450 °C for a MoO_3-WO_3 resistor.[47]

Conclusion

In this work, we built double lateral heterojunctions consisted in a low conductive sublayer, made with electroplated polymer in the emeraldine base form and a highly conductive $LuPc_2$ top layer. This device exhibited a non-linear behavior at low bias, which was consistent with the existence of interfacial energy barriers, as confirmed by the Nyquist plots. The behavior of PDMA is unique among the studied polyanilines, since it is both easily electro-polymerized and easily de-doped. The sensitivity of PDMA-DLH to NH_3 in humid atmosphere is higher than that of the PANI-DLH in all the NH_3 concentration range (1-90 ppm). This sensor operated in the full humidity range (10 % - 70 % RH) with a good baseline stability. Its calibration curve demonstrated a Langmuir adsorption behavior. The linear regime at low NH_3 concentration (< 10 ppm) permitted to deduce a sensitivity of 1.85 %.ppm^{-1}. Finally, we determined the LOD on this new device, at 320 ppb. It appears that the sensitivity to ammonia decreases when the relative humidity tends to dry atmosphere, but the LOD remains in the sub-ppm range, even at 10 % RH. It is worth noting that a RH value of 10% is rarely encountered in applications of ammonia sensors. We demonstrated a new application of conducting polymers, in their poor conducting state, as a component of lateral heterojunctions. The PDMA – based sensors were more sensitive to NH_3 than the phthalocyanine-based heterojunctions that inspired this work.

Table 1. Sensitivities (S) of the present devices compared to those of a series of heterojunctions (MSDI and DLH) and resistors.

Device (type of charge carriers)	S (% ppm^{-1})	[NH_3] (ppm)	LOD (ppm)	Ref.
Cu(F_{16}Pc)/$LuPc_2$ MSDI (n)	1.5	25		44
$LuPc_2$ resistor (p)	0.02	25		44
PTFANI – DLH (p)	1.05	1-9	0.45	21
PANI – DLH (p)	0.14	1-9	> 1	this work
PDMA – DLH (p)	1.85	1-9	0.32	this work
rGO-PANI resistor (p)	1.0 [b]	20		46
rGO-Co_3O_4 resistor (p)	1.0 [c]	50		45
MoO_3-WO_3 resistor (p)	100 [d]	5		47

a) The sensitivity drops after few days in ambient air, b) in dry air, c) at 40% RH and d) at 450 °C

ASSOCIATED CONTENT

O(1s), Cl(2p) and C(1s) XPS spectra of PDMA film; I(V) characteristics of PANI/$LuPc_2$, PDMA/$LuPc_2$ heterojunction and $LuPc_2$ resistor; Nyquist plot as a function of the bias of PANI/$LuPc_2$; variation of the circuit parameters as a function of the bias for PANI/$LuPc_2$ and response of PDMA/$LuPc_2$ to RH. This material is available free of charge via the Internet at http://pubs.acs.org.

AUTHOR INFORMATION

Corresponding Authors

Institut de Chimie Moléculaire de l'Université de Bourgogne (ICMUB), UMR CNRS 6302, Université Bourgogne Franche-Comté, 9 av. Alain Savary, 21078 Dijon cedex, France. Tel: +33-380-396-086; E-mail: marcel.bouvet@u-bourgogne.fr, rita.meunier-prest@u-bourgogne.fr

Author Contributions

All authors have given approval to the final version of the manuscript.

ACKNOWLEDGMENT

The authors acknowledge the *Agence Nationale de la Recherche* for funding through the ANR project OUTSMART ANR-2015-CE39-0004-03 and the MENESR for a PhD grant (M. M.). Financial support from the European Union (FEDER) and the *Conseil Régional de Bourgogne* through the FABER and the CDEA program is gratefully acknowledged. We also acknowledge the *Conseil Régional de Bourgogne* through the CPER program.

REFERENCES

(1) de Gans, B. J.; Duineveld, P. C.; Schubert, U. S. Inkjet Printing of Polymers: State of the Art and Future Developments. *Adv. Mater.* **2004**, *16* (3), 203–213.

(2) Ha, J.; Chung, S.; Pei, M.; Cho, K.; Yang, H.; Hong, Y. One-Step Interface Engineering for All-Inkjet-Printed, All-Organic Components in Transparent, Flexible Transistors and Inverters: Polymer Binding. *ACS Appl. Mater. Interfaces* **2017**, *9* (10), 8819–8829.

(3) Miller, D. R.; Akbar, S. A.; Morris, P. A. Nanoscale Metal Oxide-Based Heterojunctions for Gas Sensing: a Review. *Sens. Actuators: B. Chem.* **2014**, *204*, 250–272.

(4) Dhawale, D. S.; Dubal, D. P.; More, A. M.; Gujar, T. P.; Lokhande, C. D. Room Temperature Liquefied Petroleum Gas (LPG) Sensor. *Sens. Actuators: B. Chem.* **2010**, *147* (2), 488–494.

(5) Xiao, Y.; Yang, Q.; Wang, Z.; Zhang, R.; Gao, Y.; Sun, P.; Sun, Y.; Lu, G. Improvement of NO_2 Gas Sensing Performance Based on Discoid Tin Oxide Modified by Reduced Graphene Oxide. *Sens. Actuators: B. Chem.* **2016**, 227, 419–426.

(6) Geng, L.; Zhao, Y.; Huang, X.; Wang, S.; Zhang, S.; Wu, S. Characterization and Gas Sensitivity Study of Polyaniline/SnO_2 Hybrid Material Prepared by Hydrothermal Route. *Sens. Actuators: B. Chem.* **2007**, *120* (2), 568–572.

(7) Xu, M.; Zhang, J.; Wang, S.; Guo, X.; Xia, H.; Wang, Y.; Zhang, S.; Huang, W.; Wu, S. Gas Sensing Properties of SnO_2 Hollow Spheres/Polythiophene Inorganic–Organic Hybrids. *Sens. Actuators: B. Chem.* **2010**, *146* (1), 8–13.

(8) Ebrahimiasl, S.; Zakaria, A. Electrochemical Synthesis, Characterization and Gas Sensing Properties of Hybrid Ppy/CS Coated ZnO Nanospheres. *Int. J. Electrochem. Sci.* **2016**, 9902–9916.

(9) Hatchett, D. W.; Josowicz, M. Composites of Intrinsically Conducting Polymers as Sensing Nanomaterials. *Chem. Rev.* **2008**, *108* (2), 746–769.

(10) Chowdhury, A.; Biswas, B.; Bera, R. N.; Mallik, B. Nanostructured Organic–Inorganic Heterojunction Diodes as Gas Sensors. *RSC Advances* **2012**, *2* (29), 10968–10976.

(11) Potje-Kamloth, K. Semiconductor Junction Gas Sensors. *Chem. Rev.* **2008**, *108* (2), 367–399.

(12) Muzikante, I.; Parra, V.; Dobulans, R.; Fonavs, E.; Latvels, J.; Bouvet, M. A Novel Gas Sensor Transducer Based on Phthalocyanine Heterojunction Devices. *Sensors* **2007**, *7* (11), 2984–2996.

(13) Parra, V.; Brunet, J.; Pauly, A.; Bouvet, M. Molecular Semiconductor-Doped Insulator (MSDI) Heterojunctions: an Alternative Transducer for Gas Chemosensing. *Analyst* **2009**, *134* (9), 1776–1778.

(14) Parra, V.; Bouvet, M. Semiconductor Transducer and Its Use in a Sensor for Detecting Electron-Donor or Electron-Acceptor Species, US8450725 B2, 2013-05-28.

(15) Yan, M.; Kawamata, Y.; Baran, P. S. Synthetic Organic Electrochemical Methods Since 2000: on the Verge of a Renaissance. *Chem. Rev.* **2017**, *117* (21), 13230–13319.

(16) Bélanger, D.; Pinson, J. Electrografting: a Powerful Method for Surface Modification. *Chem. Soc. Rev.* **2011**, *40* (7), 3995–4048.

(17) Sizun, T.; Patois, T.; Bouvet, M.; Lakard, B. Microstructured Electrodeposited Polypyrrole–Phthalocyanine Hybrid Material, From Morphology to Ammonia Sensing. *J. Mater. Chem.* **2012**, *22* (48), 25246–25248.

(18) Epstein, A. J.; MacDiarmid, A. G. Polyaniline Versus Polyacetylene, or, Rings Versus Bonds and the Roles of Barriers and Crystallinity. In *Conjugated Polymeric Materials: Opportunities in Electronics, Optoelectronics, and Molecular Electronics;* Brédas, J. L., Chance, R. R., Eds.; Springer Netherlands: Dordrecht, 1990; pp 195–205.

(19) Cihaner, A.; Önal, A. M. Electrochemical Behaviour and Electrochemical Polymerization of Fluoro-Substituted Anilines. *Polym. Int.* **2002**, *51* (8), 680–686.

(20) D'Aprano, G.; Leclerc, M.; Zotti, G.; Schiavon, G. Synthesis and Characterization of Polyaniline Derivatives: Poly(2-Alkoxyanilines) and Poly(2,5-Dialkoxyanilines). *Chem. Mater.* **1995**, *7* (1), 33–42.

(21) Mateos, M.; Meunier-Prest, R.; Heintz, O.; Herbst, F.; Suisse, J.-M. Comprehensive Study of Poly(2,3,5,6-Tetrafluoroaniline): From Electrosynthesis to Heterojunctions and Ammonia Sensing. *ACS Appl. Mater. Interfaces* **2018**, *10*, 19974–19986.

(22) Kirin, I. S.; Moskalev, P. N.; Makashev, Y. A. Formation of Unusual Phthalocyanines of the Rare-Earth Elements. *Russ. J. Inorg. Chem.* **1965**, *10*, 1065–1066.

(23) Wagner, C. D.; Riggs, W. M.; Davis, L. E.; Moulder, J. E.; Muilenber, G. E. *Handbook of X-Ray Photoelectron Spectroscopy;* Perkin Elmer Corporation Physical Electronics Division: USA, 1979.

(24) Gaudillat, P.; Wannebroucq, A.; Suisse, J.-M.; Bouvet, M. Bias and Humidity Effects on the Ammonia Sensing of Perylene Derivative/Lutetium Bisphthalocyanine MSDI Heterojunctions. *Sens. Actuators: B. Chem.* **2016**, *222*, 910–917.

(25) Storrier, G. D.; Colbran, S. B.; Hibbert, D. B. Chemical and Electrochemical Syntheses, and Characterization of Poly(2,5-Dimethoxyaniline) (PDMA) - a Novel, Soluble, Conducting Polymer. *Synth. Met.* **1994**, *62* (2), 179–186.

(26) Palys, B.; Kudelski, A.; Stankiewicz, A.; Jackowska, K. Influence of Anions on Formation and Electroacitivity of Poly-2,5-Dimethoxyaniline. *Synth. Met.* **2000**, *108* (2), 111–119.

(27) Suephatthima, B.; Paradee, N.; Sirivat, A.; Pattavarakorn, D. Effect of Electrolytes on Electrochromic Properties and Morphology of Poly(2,5-Dimethoxy Aniline) Films. *Bull. Mater. Sci.* **2014**, *37* (5), 975–982.

(28) Amin, M. A. Metastable and Stable Pitting Events on Al Induced by Chlorate and Perchlorate Anions—Polarization, XPS and SEM Studies. *Electrochim. Acta* **2009**, *54* (6), 1857–1863.

(29) Han, C.-C.; Chen, H.-Y. Highly Conductive and Electroactive Fluorine-Functionalized Polyanilines. *Macromol.* **2007**, *40* (25), 8969–8973.

(30) Neoh, K. G.; Kang, E. T.; Tan, K. L. Thermal Degradation Studies of Perchlorate-Doped Conductive Polymers. *J. Appl. Polym. Sci.* **1991**, *43* (3), 573–579.

(31) Kang, E. T.; Neoh, K. G.; Tan, K. L. The Intrinsic Redox States in Polypyrrole and Polyaniline: a Comparative Study by XPS. *Surf. Inter. Anal.* **1992**, *19* (1-12), 33–37.

(32) Wei, X. L.; Fahlman, M.; Epstein, A. J. XPS Study of Highly Sulfonated Polyaniline. *Macromol.* **1999**, *32* (9), 3114–3117.

(33) Sui, J.; Zhang, L.; Peng, H.; Travas-Sejdic, J.; Kilmartin, P. A. Self-Assembly of Poly(o-Methoxyaniline) Hollow Nanospheres From a Polymeric Acid Solution. *Nanotechnology* **2009**, *20* (41), 415606.

(34) Hasik, M.; Wenda, E.; Paluszkiewicz, C.; Bernasik, A.; Camra, J. Poly(o-Methoxyaniline)–Palladium Systems: Effect of Preparation Conditions on Physico-Chemical Properties. *Synth. Met.* **2004**, *143* (3), 341–350.

(35) Kuwabara, T.; Kawahara, Y.; Yamaguchi, T.; Takahashi, K. Characterization of Inverted-Type Organic Solar Cells with a ZnO Layer as the Electron Collection Electrode by AC Impedance Spectroscopy. *ACS Appl. Mater. Interfaces* **2009**, *1* (10), 2107–2110.

(36) Kim, C.-H.; Hlaing, H.; Yang, S.; Bonnassieux, Y.; Horowitz, G.; Kymissis, I. Impedance Spectroscopy on Copper Phthalocyanine Diodes with Surface-Induced Molecular Orientation. *Org. Electron.* **2014**, *15* (8), 1724–1730.

(37) Bouvet, M.; Gaudillat, P.; Kumar, A.; Sauerwald, T.; Schüler, M.; Schütze, A.; Suisse, J.-M. Revisiting the Electronic Properties of Molecular Semiconductor – Doped Insulator (MSDI) Heterojunctions Through Impedance and Chemosensing Studies. *Org. Electron.* **2015**, *26*, 345–354.

(38) Miller, K. A.; Yang, R. D.; Hale, M. J.; Park, J.; Fruhberger, B.; Colesniuc, C. N.; Schuller, I. K.; Kummel, A. C.; Trogler, W. C. Electrode Independent Chemoresistive Response for Cobalt Phthalocyanine in the Space Charge Limited Conductivity Regime. *J. Phys. Chem. B* **2006**, *110* (1), 361–366.

(39) Braga, D.; Campione, M.; Borghesi, A.; Horowitz, G. Organic Metal-Semiconductor Field-Effect Transistor (OMESFET) Fabricated on a Rubrene Single Crystal. *Adv. Mater.* **2010**, *22* (3), 424–428.

(40) Raistrick, I. D.; Franceschetti, D. R.; MacDonald, J. R. Theory. In *Impedance Spectroscopy;* Barsoukov, E., MacDonald, J. R., Eds.; Theory, Experiment, and Applications; John Wiley & Sons, Inc.: Hoboken, NJ, USA, 2005; pp 27–128.

(41) Hsu, C. H.; Mansfeld, F. Technical Note: Concerning the Conversion of the Constant Phase Element Parameter Y0 Into a Capacitance. *Corrosion* **2001**, *57* (9), 747–748.

(42) Chung, M. G.; Kim, D. H.; Lee, H. M.; Kim, T.; Choi, J. H.; Seo, D. K.; Yoo, J.-B.; Hong, S.-H.; Kang, T. J.; Kim, Y. H. Highly Sensitive NO_2 Gas Sensor Based on Ozone Treated Graphene. *Sens. Actuators: B. Chem.* **2012**, *166-167*, 172–176.

(43) Directive 2008/50/EC of the European Parliament and of the Council of 21 May 2008, on Ambient Air Quality and Cleaner Air for Europe; 2008; Vol. L 152, pp 1–44.

(44) Bouvet, M.; Gaudillat, P.; Suisse, J.-M. Lanthanide Macrocyclic Complexes: From Molecules to Materials and From Materials to Devices. *J. Porphyrins Phthalocyanines* **2013**, *17*, 628–635.

(45) Feng, Q.; Li, X.; Wang, J.; Gaskov, A. M. Reduced Graphene Oxide (rGO) Encapsulated Co_3O_4 Composite Nanofibers for Highly Selective Ammonia Sensors. *Sens. Actuators: B. Chem.* **2016**, *222*, 864–870.

(46) Huang, X. L.; Hu, N. T.; Wang, Y. Y.; Zhang, Y. F. Ammonia Gas Sensor Based on Aniline Reduced Graphene Oxide. *Adv. Mater. Res.* **2013**, *669*, 79–84.

(47) Xu, C. N.; Miura, N.; Ishida, Y.; Matsuda, K.; Yamazoe, N. Selective Detection of NH_3 Over NO in Combustion Exhausts by Using Au and MoO_3 Doubly Promoted WO_3 Element. *Sens. Actuators: B. Chem.* **2000**, *65* (1-3), 163–165.